

Etch-Pit Observations of Dislocation Arrangements under Reverse Stress in Copper 9 at. % Aluminum Alloy Single Crystals

By

Satoshi HASHIMOTO and Sei MIURA

(Received June 27, 1985)

Abstract

With a view of solving the cause and essence of the Bauschinger effect, dislocation behaviour under reverse stress has been investigated in Cu-9at% Al alloy single crystals, using an etch-pitting technique. From the direct measurements of the beginnings of backward movements of dislocations, the frictional resistance force to moving dislocations due to solid solution hardening is estimated to be approximately 0.8 kg/mm^2 , which is $\simeq 4/5$ of easy glide stress. It is found that pile-up dislocations against a barrier move well under the reverse stress range from 0.6 to 0.7 to the pre-stress level, but then hardly move more than the reverse stress ratio of 0.8. Evidence of almost complete annihilation of double ended pile-ups which are generated by the same source is presented. Another striking evidence of radical annihilation of dislocations within uniformly aligned dislocation groups of the same sign is also discovered. Mechanisms acceptable for explaining such results are proposed respectively, i. e., the mutual annihilation of dislocations of opposite signs, and the double cross-slip mechanism. It is suggested that the characteristics of rearrangements of dislocations against stress reversal are probably connected with the latter mechanism, which would be responsible for cyclic strain hardening.

1. Introduction

The dislocation arrangements and movements which occur in reverse deformation are of considerable interest, because they are the ultimate cause of the Bauschinger effect. They are also closely related to the mechanism of cyclic strain hardening. There has been relatively little work¹⁻³⁾ on dislocation behaviour under reverse stress. In particular, on follow-up surveys of identical dislocations in the same specimen when the specimen is subjected to the pre-stress level, it has been carried out in copper. Vellaikal¹⁾ has examined the motion of dislocation pile-ups generated by a strain well below the macroscopic yield stress in large grained polycrystalline copper. It was found that the movement of primary dislocations under reverse stress was

Department of Engineering Science, Faculty of Engineering, Kyoto University, Kyoto-606, Japan

suppressed owing to the interaction with the dislocations generated from a secondary source. It was also found that dislocations in a pile-up never collapsed completely back to the source on stress reversal. Daniel and Horne³⁾, and Marukawa and Sanpei³⁾ have investigated the rearrangements of dislocations under reverse stress in a copper single crystal by an etch-pitting technique. They observed that only relatively inhomogeneous distributions, such as kink bands or dislocation walls and glide polygonizations, which may be associated with the local bending of the specimen, disappear during reverse stress.

The importance of the stacking-fault energy of metals on work hardening behaviour has long been recognized. The equilibrium separation of partial dislocations is determined by the stacking-fault energy. Cross slipping of the partials is difficult if they are widely separated, as in the case of metals with low stacking-fault energy. The stacking-fault energies of alloys of the Cu-Al system have been studied by some investigators⁴⁻⁷⁾. The results indicate that the energy decreases from 70 ergs/cm² for pure Cu to about 2 ergs/cm² with increasing additions of Al in the fcc alpha-solid solution. The value of the present Cu-9at. %Al is about 6 ergs/cm².

Extensive studies⁸⁻¹⁰⁾ have been performed with Cu and Cu-Al alloys by transmission electron microscopy to compare the characteristics of dislocation distributions with strain due to the difference of stacking-fault energy. It was found that the most prominent distributions of pure Cu are mainly characterized by a three dimensional or "wavy" slip mode. On the other hand, those of a high concentration α Cu-Al alloy having an extremely low value of energy are mainly regarded as a two dimensional or "planar" slip mode.

The relative ease of cross slip of screw dislocations also affects the distributions of dislocations as well as the strain hardening behaviour in fcc metals subjected to fatigue deformation. The degree of cell formation and size are directly related to the stacking-fault energy of the metals¹¹⁻¹³⁾. Also, metals having a low stacking-fault energy harden at lower rates than those of higher stacking-fault energy¹⁴⁾.

Therefore, in order to clarify the mechanism of the Bauschinger effect or cyclic strain hardening of metals having a low stacking-fault energy, one would expect direct observations of dislocation arrangements and the behaviour of dislocations during reverse stress in Cu-Al alloy single crystals. Fortunately, an etch pitting technique has been employed successfully to reveal such dislocations¹⁶⁻¹⁸⁾. As far as we know, however, this kind of observation seems to be almost unexplored. The purpose of the experiments described in this paper is to observe, by an etch pitting technique, the behaviour of dislocations under reverse stress in Cu-9at. %Al single crystals deformed to the small strain just beyond yielding.

2. Experimental Procedures

An alloy of Cu-9.2at. %Al was supplied by the Sumitomo Light Metal Co. Ltd., prepared by a vacuum melting of the base elements of OFHC copper and 99.99% purity Al. The chemical analysis of the alloy is shown in Table 1.

Table 1. Chemical analysis of the alloy used.

Element	Copper	Aluminium	Iron	Lead
wt. %	95.57	4.10	<0.01	<0.01

Oriented single crystals about 20 cm in length and with square cross sections ($4 \times 18 \text{ mm}^2$) were grown from the seed in graphite moulds by the Bridgman method under a dynamic vacuum of 10^{-5} torr or better with a 2 cm/h growth rate. The crystals grown had growth direction and a tensile axis $[431]$. Also, they had a pair of surfaces parallel to the $(1\bar{1}\bar{1})$ cross slip plane within $\pm 1.5^\circ$, determined from back-reflection Laue X-ray diffraction patterns. Figure 1 shows the crystallographic geometry of the specimen. The cross slip plane $(1\bar{1}\bar{1})$ is parallel to two specimen surfaces, and is used for etching. Since the slip direction \mathbf{b} of the primary slip

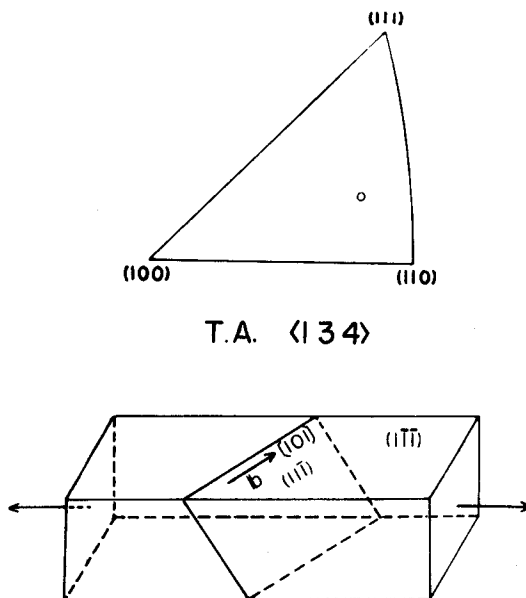


Fig. 1. Stereographic projection of the crystallographic orientation of the specimen and geometry of the primary slip plane $(1\bar{1}\bar{1})$, relative to the crystal surfaces of cross slip plane $(1\bar{1}\bar{1})$ and tensile axis.

direction $(1\bar{1}\bar{1})$ $[101]$ lies on the observation surface, pits are produced almost by the edge dislocations of the primary system.

The crystals were then cut into parallelepipeds measuring $4 \times 8 \times 35$ mm³ using a spark-cutter knife attachment. Each crystal was subsequently spark cut using a pair of brass blades machined with accuracy to shape a gauge length part. The final shape of the specimen used in the experiment is shown in Fig. 2, where the gauge length L is 12 mm, the width W is about 4 mm and the thickness H is about 3.5 mm respectively.

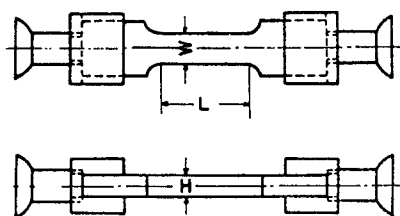


Fig. 2. Schematic drawing of the specimen used. The gauge length L is 12 mm, the width W is about 4 mm and the thickness H is about 3.5 mm respectively.

The shaped specimens were cyclic-annealed for one week between 800°C to 1040°C by periodically switching the current of a heating furnace on and off in a dynamic vacuum of less than 10^{-4} torr. By this treatment, consequently, the dislocation density was reduced from about 1×10^8 /cm² for as-grown crystals to $1 \times 10^4 \sim 2 \times 10^5$ /cm², and the average sub-grain diameter increased from 0.2 mm to 1~3 mm.

The specimens were then polished on 600, 800 and 1200 grit papers to remove surface roughness. Smooth etchable surfaces were produced by electropolishing in a solution of 80% orthophosphoric acid and 20% ethyl alcohol with DISA Electropol. After electropolishing, a sequence of the surface preparation similar to that introduced by Mitchell et al.¹⁶⁾ was employed.

A modified Livingston's etchant¹⁹⁾ for Cu-Al alloy by Yoshioka et al.¹⁸⁾ was employed to reveal dislocations on the $(1\bar{1}\bar{1})$ surface. The composition of the etchant was 1 cc of bromine, 20 cc of glacial acetic acid, 60 cc of hydrochloric acid and 100 cc of distilled water. The etching temperature was usually controlled at 0~5°C, and the standard etching time ranged from 5~30 sec. As-etched surfaces were rinsed thoroughly in running water and dried with a cool-air drier. The specimens were etched in a stress-released condition after unloading. Optical micrographs were taken on a Nikon-R differential interference microscope.

The mechanical testing was performed at room temperature on an Instron type testing machine at a cross-head speed of 0.05 mm/min. The change of the loading

direction was attained simply by the combination of uniaxial tension and compression. For the tension, small ball joints screwed in brass blocks soldered to both shoulders of the specimen were employed, whereas compression was achieved directly with these parallel blocks by taking off the ball joints. (See Fig. 2.) The stress-strain curves were computed from load-time data, and no measurement of microstrain was attempted.

3. Results and Discussion

3.1. Features of dislocation distributions just after yielding

The specimens were initially stressed in compression until the yield point was recognized in a load-time chart and then unloaded. Narrow slip bands on two lateral planes were observed at the same time as the yielding by an examination using a magnifying glass. The critical resolved shear stresses on the primary glide system at the yield point ranged from 1.0 to 1.1 kg/mm², which are considered to be reasonable values compared with those of 1.05 kg/mm² obtained by Pande and Hazzledine⁹⁾ in Cu-10 at%Al single crystals.

Figure 3 shows the distribution of etch pits in the form of bands on the (1 $\bar{1}\bar{1}$) plane, (a), (c); and the corresponding slip lines produced on the lateral face, (b), (d). The directions of the intersection of primary and cross-slip planes with the lateral plane are indicated in the figure. As can be seen, the cross-slip of primary dislocations takes place from the beginning of deformations, in spite of no shear stress on the cross-slip plane, due to the applied stress in the case of the present crystal orientation.

Figure 4 shows a typical band structure just after yielding at low magnification. In the figure, both single-ended and double-ended pile-ups are observed, but the well-defined double-ended pile-ups are not common in the present observations. Some activations of secondary slip systems are also observed in and near the bands, and increase with the width of the band with increasing strain. Sub-boundaries act as obstacles to the motion of dislocations, but these do not impede the relatively long range motion of the primary dislocations. It appears that these do not prevent the development of the bands. The motion and multiplication of grown-in dislocations or freshly generated dislocations have never been observed before yielding, neither by examination of etch pitting nor slip lines.

Typical distributions of dislocations within the deformation band are shown in Fig. 5. The general features of dislocation distributions were similar to the observations of Mitchell et al.¹⁶⁾ and Hockey and Mitchell¹⁷⁾. They are summarized as follows: The band is almost totally composed of single-ended pile-ups and rows of more densely packed pits on a single glide plane, which cannot be resolved to

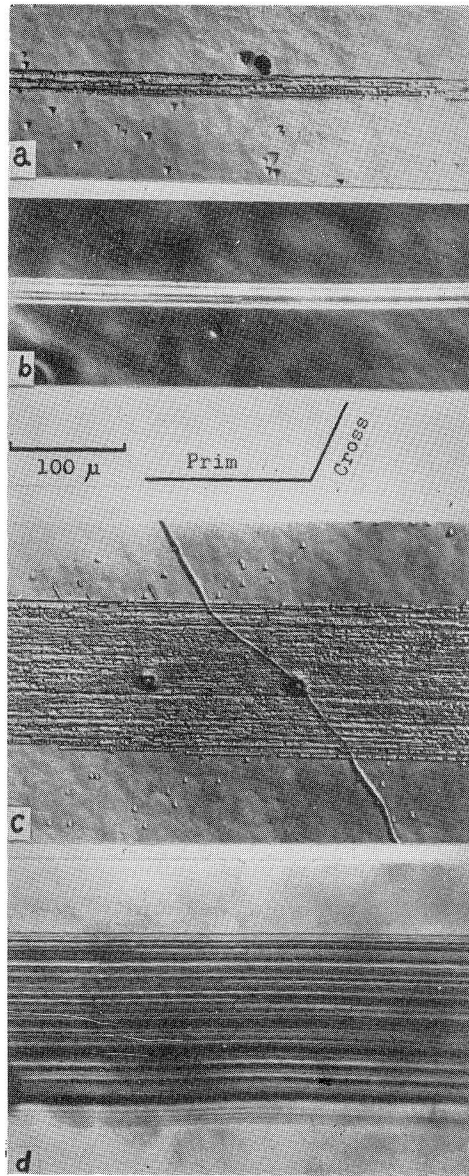


Fig. 3. Macroscopic photographs showing distributions of etch pits in the form of deformation band on (111) plane, (a)(c), and the corresponding slip markings produced on the lateral plane, (b)(d) just beyond yielding. Prim. and Cross. identify traces of primary and cross slip planes on the lateral plane.

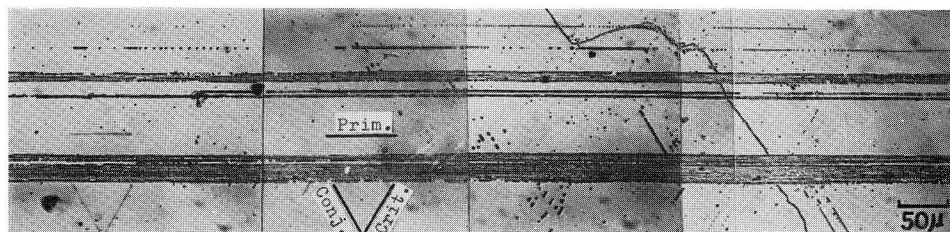


Fig. 4. Etched $(1\bar{1}\bar{1})$ surface showing primary pile-ups and deformation bands after yielding.

individual pits at this magnification. The mean separation is usually $1\sim 2\ \mu\text{m}$. The alternate arrays, which are commonly considered to be dislocations having opposite signs of the Burgers vectors on an adjacent glide plane are also seen by the characteristic light and dark pits^{16,17,20}.

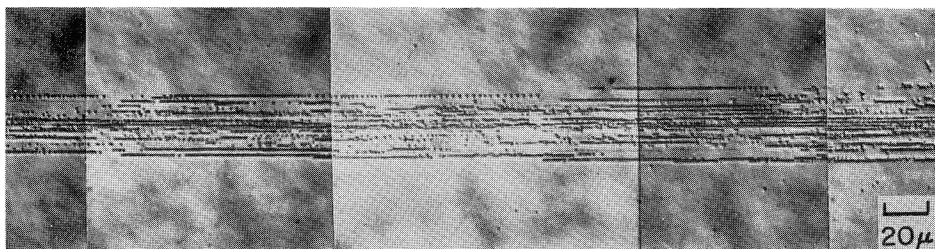


Fig. 5. Etched $(1\bar{1}\bar{1})$ surface showing typical distributions of etch pits within a deformation band.

The dislocations within a narrow band, which are composed of two or three arrays of pile-ups, are more likely to be piled up in the opposite direction. Also, they are more likely to form dipoles by pairs of opposite signs on adjacent glide planes when the separation of the glide planes is approximately equal to the spacing of dislocations along them, as shown in Fig. 6.

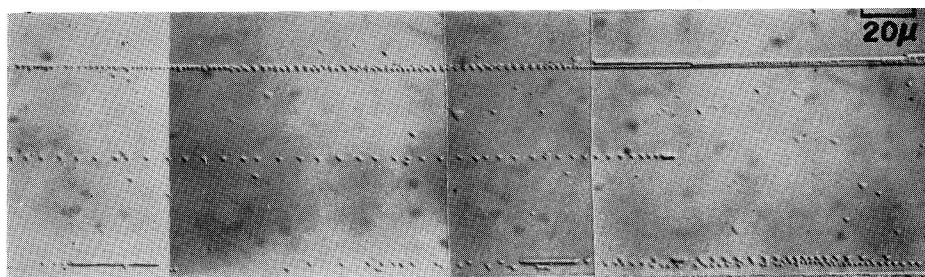


Fig. 6. Dipole formed by pairs of dislocations of opposite signs on adjacent glide planes.

3.2. The mobility of dislocations during reverse stressing

In the first place, in order to examine the reversibility of slip lines under the subsequent reverse tensile stressing, the slip steps produced during the pre-stressing were erased by electropolishing. Slip lines were not observed to the extent of reverse stress ratio, τ_R/τ_p , of 0.5. Newly generated slip lines were again observed at the ratio of 0.6 in the positions where the previous lines were located, namely where τ_R is the reverse stress and τ_p is the pre-stress. The results of the slip line reversibility are consistent with the observations, in that no change of etch-pit configurations was recognized at the reverse stress ratio of 0.5. However, at the ratio of 0.6, the motion of almost all dislocations was observed from the double etch-pit results. The etch-pit photographs showing this examination by the double etching method will be presented later, e. g., in Figs.9 and 10. From these results it is concluded that the dislocations generated during pre-strain begin to move at the reverse stress, which ranged from 0.5 to 0.6 kg/mm², and this caused a reverse 'slipping' of slip lines. This is in accordance with the observations of Cu-12.5 at% Al by Charsley and Desvaux²¹⁾, that slip steps which are formed during tensile pre-strain become smaller after a subsequent compressive strain using a highly resolved replica technique.

Cottrell²²⁾ has described a simple method for determining the frictional stress on glide dislocations in deformed crystals. It is assumed that dislocations attain equilibrium under an applied stress, τ_1 , such that

$$\tau_1 = \tau_F + \tau_G, \quad (1)$$

where τ_F is the dislocation frictional stress and τ_G is the stress opposing dislocation motion due to elastic interactions. On unloading or reverse loading, the dislocations will glide in a backward direction when

$$\tau_G = \tau_2 + \tau_F, \quad (2)$$

where τ_2 is the stress corresponding to the first departure from the elastic portion of the reverse loading curve. It follows from (1) and (2) that

$$\tau_1 - \tau_2 = 2\tau_F. \quad (3)$$

Thus, a value for the frictional stress can be obtained merely by noting the difference between τ_1 and τ_2 . For the etch pit study, τ_2 must correspond to the stress at which the first dislocation movement can be detectable. Therefore, from the present results of both the slip line reversibility and the etch pit observations, the value of the frictional stress of the present alloy is estimated to be about 0.8 kg/mm². This is a reasonable value compared with that of 0.8~0.88 kg/mm² obtained by Meakin and Wildorf²³⁾, Strutt²⁴⁾ and Strutt et al.²⁵⁾ in α -brass single crystals by measurements using a high sensitivity extensometer and an elastic stress-strain loop method.

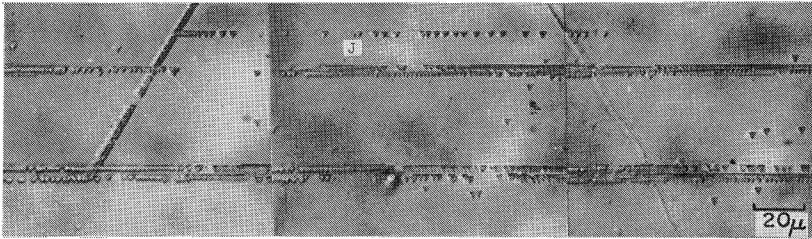
The movement and behaviour of dislocations were observed by a double etch-pit method, i. e., a large pit having a flat bottom and a small pit having a sharp apex indicated the intersection site of a dislocation which was situated in a previous stress range. Also indicated was one that occupied a new position during the subsequent loading. After the observation of etch pit arrays, a thickness about $10\ \mu\text{m}$ was usually removed from the surface by electropolishing to erase the pits. After that, the specimen was again etched for the following reverse loading. The sequence was performed successively in each stage of reverse loading. The movement of dislocation groups or individual dislocations, which are revealed as more complex and closely spaced arrays within bands, was not confirmed sufficiently due to their over-lapping. Therefore, most observations in the present investigation will be restricted to areas of a low dislocation density and simply distributed regions.

Figure 7 shows an example of the reverse motion of a dislocation group against the secondary dislocations in specimen No.2, which is named J. In the experiment on specimen No.2, six reverse stressings in terms of reverse stress ratio of 0.6, 0.66, 0.70, 0.72, 0.73 and 0.8 were performed. The values of the reverse stress ratio are indicated in the upper left of each micrograph. This group has well-defined pile-ups at the left of the row under the stress-released condition of pre-stressing, as can be seen in the figure. By applying the reversal of 0.66, the pile-ups moved backwards passing through the sub-boundary. In the next loading, the dislocations in this group again rearranged themselves in the same manner as pre-stressing. The dislocations did not move in the subsequent loading of 0.8. It was estimated that the total number of dislocations in the group decreased from 37 to a minimum value of 17, and again increased to about 30 at the reverse loading of 0.8.

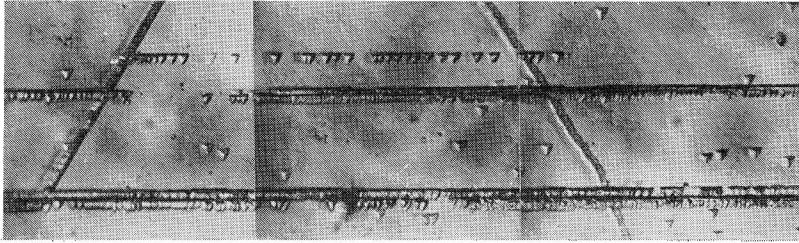
The feature of the back motion of a similar dislocation group in specimen No.2 is also shown in Fig.8. The pile-ups K and the group L, composed of rather regularly aligned pits, moved backward well after the reverse stressing of 0.66. However, the dislocations in group D were almost completely annihilated at this stress level. Some short rows which were made of faint pits were found near the band, as indicated by marks S_1 , S_2 and S_3 in the figure. It is generally considered that such dislocations are produced by a double cross-slipping of dislocations or newly multiplied by an activation of a dislocation source. Due to the limitation of geometry, it was not possible to conclude which of the two mechanisms brought about these dislocation groups which were suddenly revealed by reverse stressing. However, it is likely that there is a very fair possibility of an occurrence of cross-slipping, as will be discussed later in section 3.3.

The motions of isolated dislocation groups which commonly form single ended pile-ups were observed in detail. In Fig.9, H_p and I_p indicate the dislocation

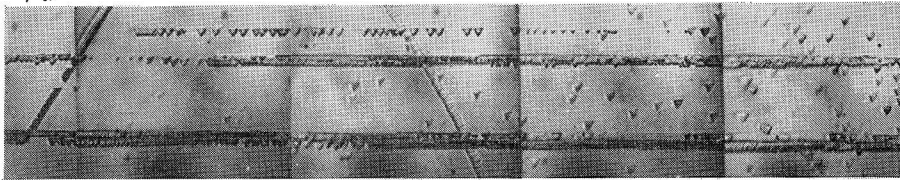
$\tau_p = 1.0 \text{ kg/mm}^2$



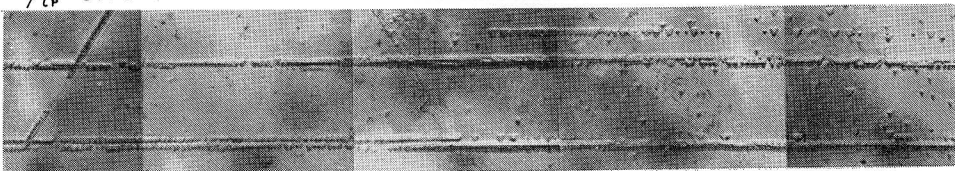
$\tau_R/\tau_p = 0.6$



$\tau_R/\tau_p = 0.66$



$\tau_R/\tau_p = 0.73$



$\tau_R/\tau_p = 0.8$

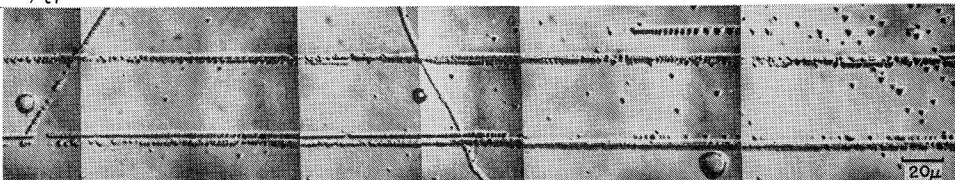


Fig. 7. Motions of dislocation group J during reverse stressing in specimen No. 2. Values of pre-stress, τ_p , and reverse stress ratio τ_R/τ_p are indicated in the upper left of each photograph.

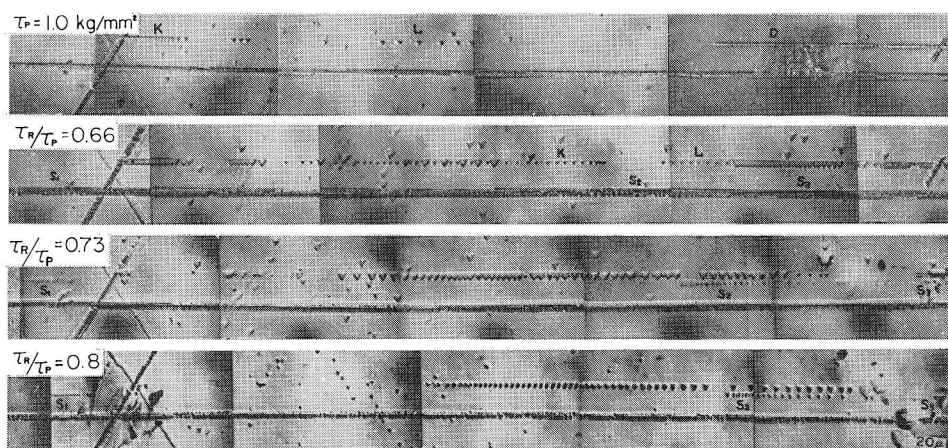


Fig. 8. Behaviour of pile-ups K and dislocation group L, D during reverse stressing in specimen No.2. Dislocation group S1, S2 and S3 newly generated under reverse stressing are seen.

intersection sites after pre-stressing. H_r and I_r indicate those newly occupied when the reverse loading of 0.6 was applied. The significant feature of these reverse motions is that they can move backwards while keeping their distribution style, if there are no barriers such as sub-boundary or forest dislocations behind the groups. In Fig. 10, point F will serve as a reference of the identical position in each photograph. The dislocation group named M moved well up to the first half of the reverse stressing. However, it was found that they moved scarcely at all under a reverse stressing of more than 0.73 and consequently aligned in the same manner as originally, although the mean space between dislocations increased. The general behaviour of the group was almost the same as the pile-ups against the secondary dislocations which have been shown in Figs. 7 and 8.

In Fig. 11, the dislocations named N, which are aligned uniformly after the application of pre-stress, are rearranged into small groups separated from one another

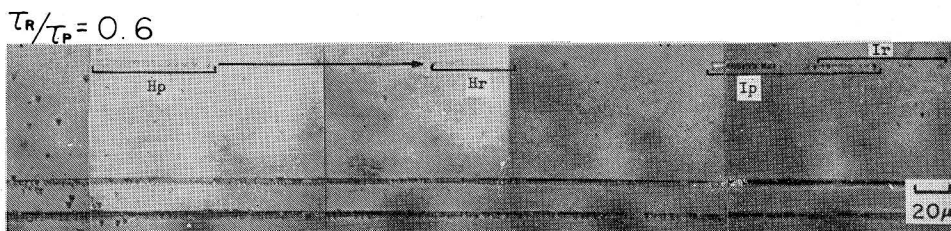


Fig. 9. Backmotion of isolated dislocation groups H and I of specimen No.2. Portions of H_p and I_p indicate the sites where these groups existed prior to reverse stressing. H_r and I_r are the positions they reach after reverse stressing of 0.6.

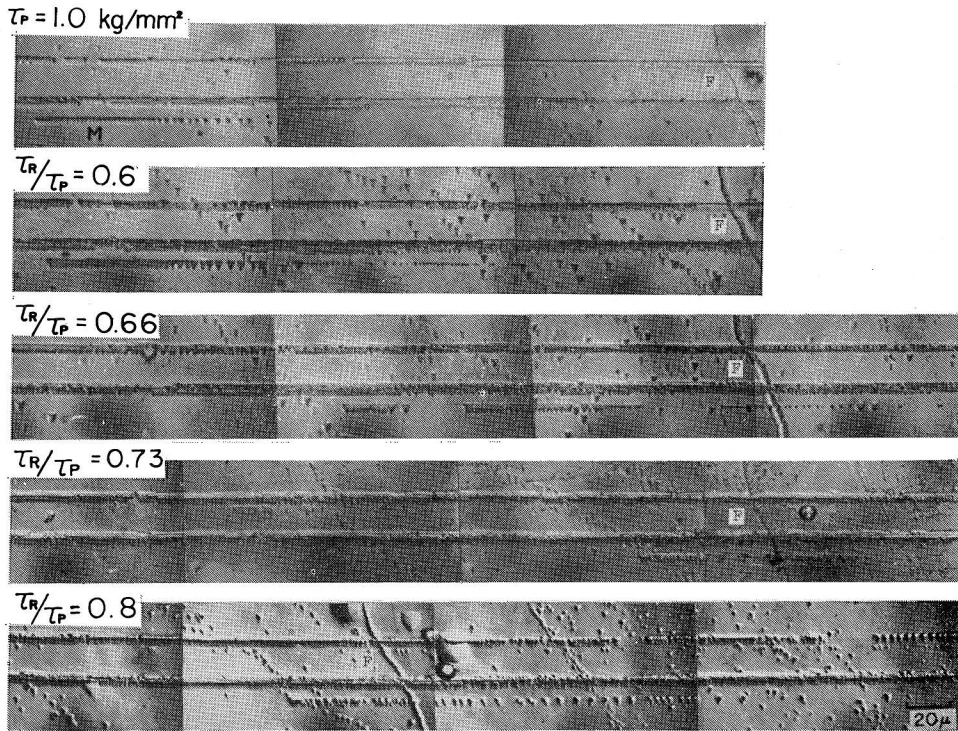
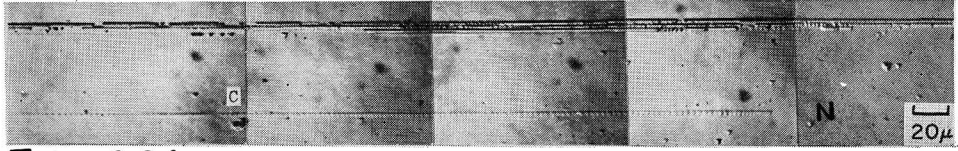


Fig. 10. Motions of isolated single ended pile-ups M during reverse stressings in specimen No. 2. Point F will serve as a reference to the identical position.

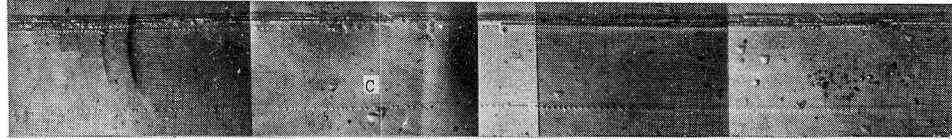
during their back motion. Point C is a reference of the identical position in each photograph. As can be seen in the third photograph (reverse stress ratio of 0.66), each group has a dark and deep pit at the trail end, and the space between the dislocations within a group shortens near the end. These facts suggest that the dislocations produced some obstacles by themselves during the back motion, because they had been able to travel all the way without obstruction, save for the head of the row, and to align uniformly during the course of pre-stressing. From these considerations, it is possible that some screw segments of the dislocation loops from inside the surface become incorporated into some attractive junctions by cross-slipping during the reverse motion. As a result, the edge segments may be retained and not be able to be aligned uniformly as revealed by etching. The behaviour and the feature of rearrangement of pile-up dislocations and isolated dislocation groups shown in Figs. 7~10 may be explained by the occurrence of this mechanism.

The distances of the reverse motion of the dislocations are plotted against the reverse stress ratio in Fig. 12. The marks in the figure correspond to each dislocation group as mentioned above. All these dislocation groups moved well up to the

$\tau_p = 1.1 \text{ kg/mm}^2$



$\tau_R/\tau_p = 0.64$



$\tau_R/\tau_p = 0.66$

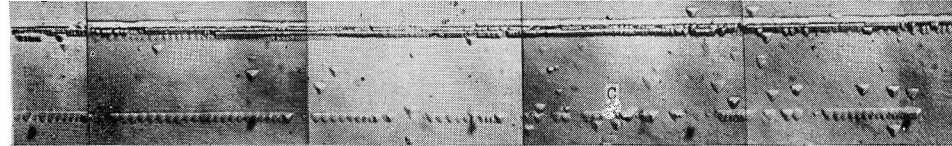


Fig. 11. Rearrangements of dislocations N during reverse stressing in No.1. Point C will serve as a reference to the identical position.

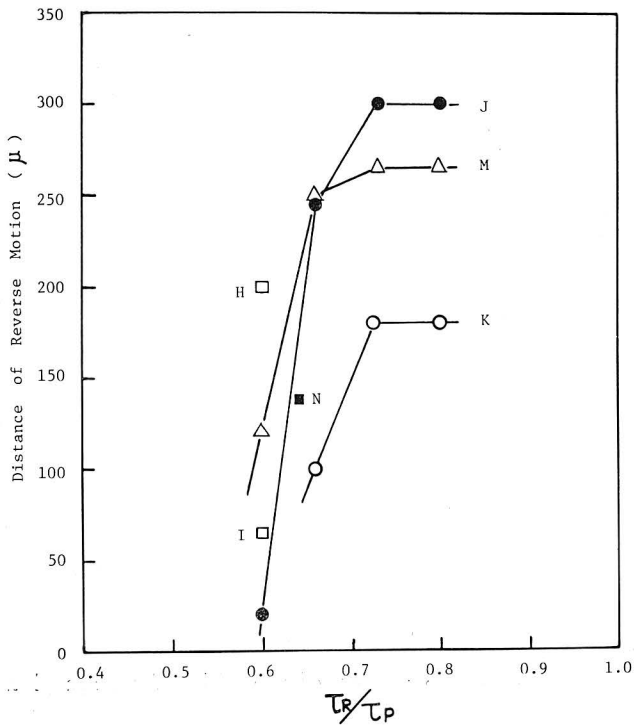


Fig. 12. Distance of reverse motion of dislocations against reverse stress ratio.

ratio of 0.7, but under the reverse stressing of more than a ratio of 0.7, they moved scarcely at all. Such behaviour does not contradict the previous statement. However, the meaning and the significance of the critical value in terms of the reverse stress ratio are not yet solved.

3.3. The annihilation and rearrangement of dislocations

An example of the occurrence of dislocation annihilation, in which the group of etch pits suddenly disappeared after the reverse stressing of about two-thirds of the pre-stress level, was demonstrated already in the previous section (at D in Fig. 8). More evidence in support of the annihilation of dislocations during reverse stressing is now given.

In Fig. 13, the short aligned dislocation group T disappeared after the reverse stressing of 0.8. As can be seen in Fig. 14, dislocation group G moved backward during the first reverse stressing, and then disappeared after the application of the reverse stress ratio of 0.8. The reason why the number of dislocations in the group increased at the reverse stress ratio of 0.65 is not known.

Figure 15 is a double etching micrograph showing the annihilation of dislocations when the specimen was subjected to the reverse stressing of 0.66. The positions of large and flat bottom pits in the rows indicate the dislocation intersection sites after the previous reverse stressing of 0.6. The most significant decrease in the number of pits which are revealed in this reverse stress range is remarkable, particularly at the rows along the upper side of the band. The rows may be

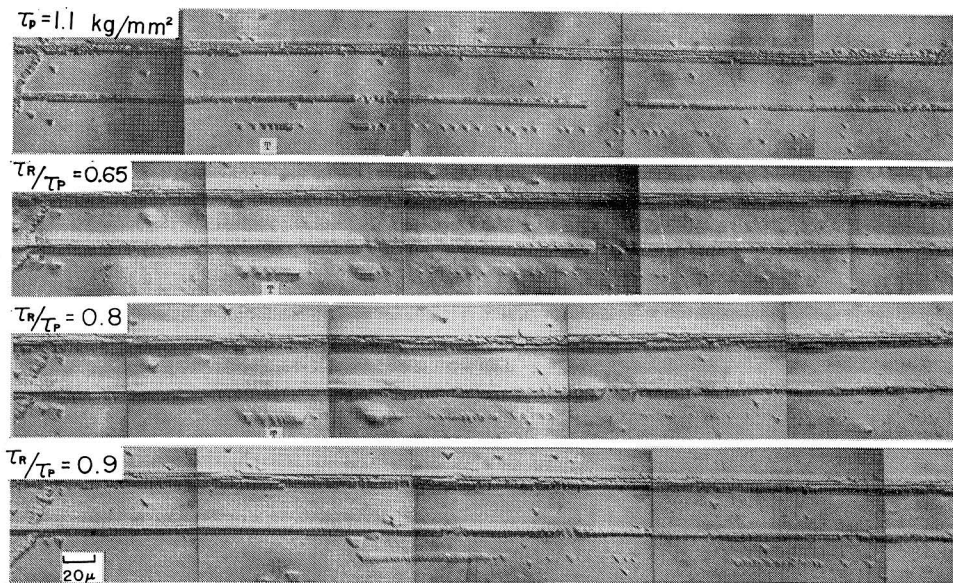


Fig. 13. Disappearance of etch-pit group T during reverse stressing in specimen No. 3.

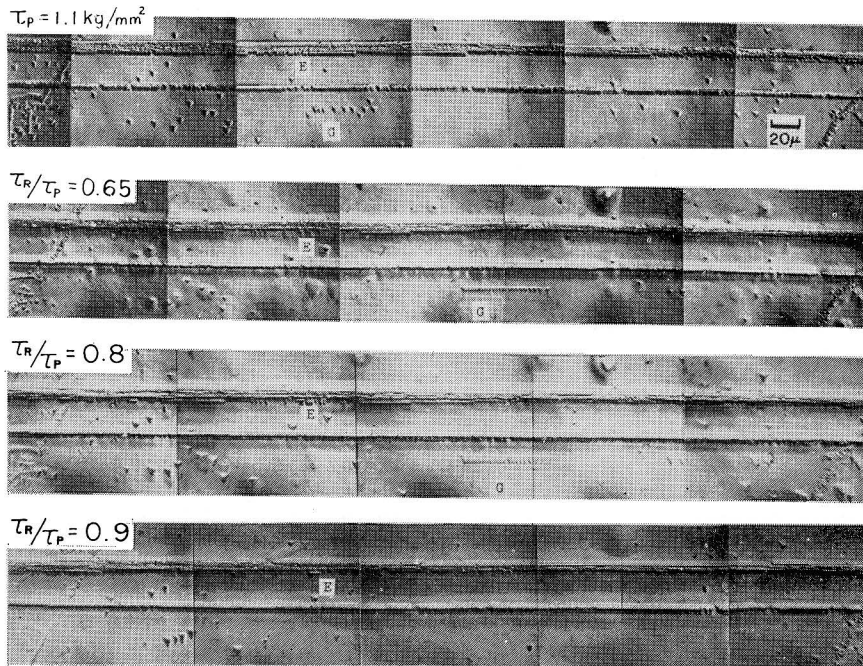


Fig. 14. Motions and annihilation of dislocation group G during reverse stressing in specimen No. 3. Point E will serve as reference to the identical position.

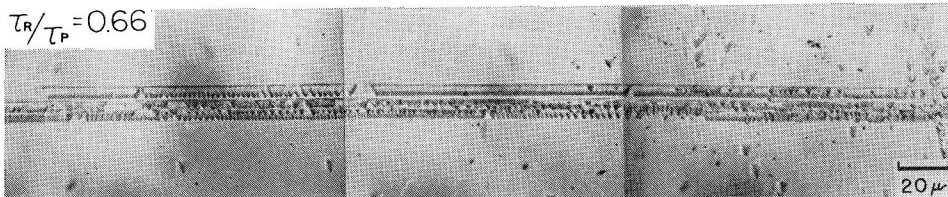


Fig. 15. Double etching micrograph showing a drastic annihilation of dislocations after reverse stressing of 0.66 in specimen No. 2.

considered to be double ended pile-ups, judging by the appearance of the distributions of the pits.

A similar feature of annihilation was observed as shown in Fig. 16. From the photograph, it was estimated that, in the upper row of the band, the etch pit density at the reverse stressing of 0.66 decreased to 45% compared with the number of pits which existed after the previous reverse stressing of 0.6. In the photograph, extremely small pits were observed among the newly revealed pits at this reverse stress stage. It may be generally considered that these pits correspond to the dislocations having less self-energy at their cores, compared with the ordinary ones. This is probably because the pit size may depend on the degree of the core energy.

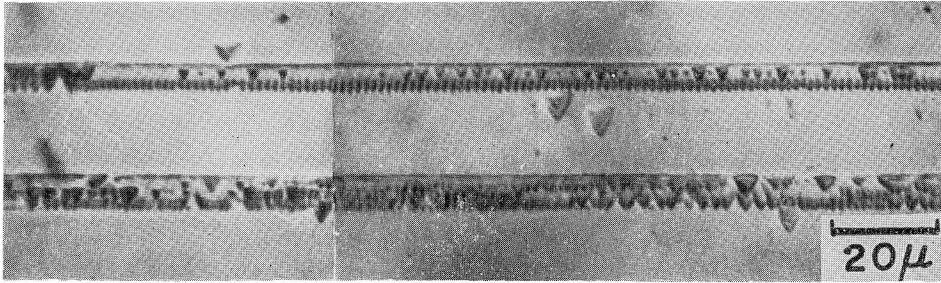


Fig. 16. Double etching micrograph showing the decrease in dislocation density after subjection to reverse stress ratio of 0.66 in specimen No.2. (See the upper row.) Extremely small pits are seen among the ordinary ones.

However, the details cannot be understood by the present observations.

A striking example of the mutual annihilation in double ended pile-ups is shown in Fig. 17. Well-defined double ended pile-ups aligned along a straight line due to the activation of the conjugate slip system were observed after the pre-stressing, as shown in (a). The upper row of pits seems to be shallower than the lower row, and the number of pits in the opposing pile-ups are almost equal to each other.

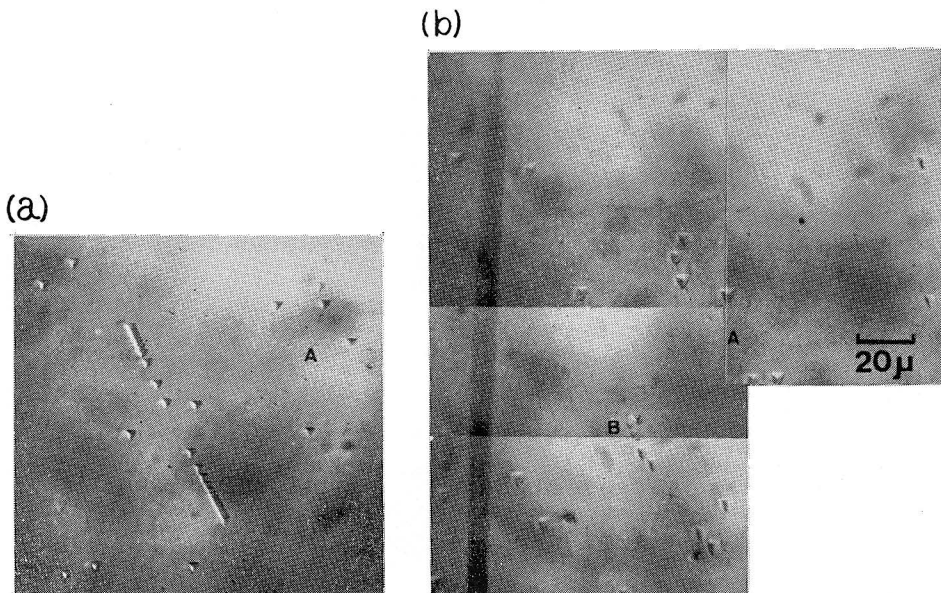


Fig. 17. An example of dislocation annihilation by operation of mutual encounters of dislocations of opposite signs in specimen No.2. Double ended pile-ups due to the activation of conjugate system in (a) almost annihilated after the application of reverse stressing in terms of reverse stress ratio of 0.6 in (b), except for a few pits at point B. Point A will serve as a reference to the former identical position.

From the distributions and the nature of the pits, it is concluded that these pile-ups correspond to positive and negative edge dislocations emitted from a single internal source of the Frank-Read type. When the specimen was subjected to the reversal of 0.6, these dislocations were almost annihilated, though a few pits still remained (near the reference point B), as can be clearly seen in Fig. 17(b).

The above demonstrations are sufficient evidence to show that some dislocations, particularly double-ended dislocation pile-ups of opposite signs of the Burgers vector, are annihilated actively during the reverse stressing in the present alloy.

The changes in dislocation density and configuration within the row composed of rather uniformly aligned pits as a function of the reverse stress ratio for specimen No.2 and No.3 were observed, and the results are shown in Figs.18 and 19, respectively. Two prominent facts were revealed by these observations. First, the annihilation of dislocations proceeded abruptly between 0.66 to 0.8 in terms of the reverse stress ratio, and then from more than the ratio of about 0.8, recovery took place. The count in the number of pits was performed within the areas outlined as indicated in each photograph. The changes in the number of pits in terms of N_R/N_P are plotted against the reverse stress ratio, as shown in Fig. 20, where N_R and N_P are the number of pits at each reversal prior to reverse stressing, respectively.

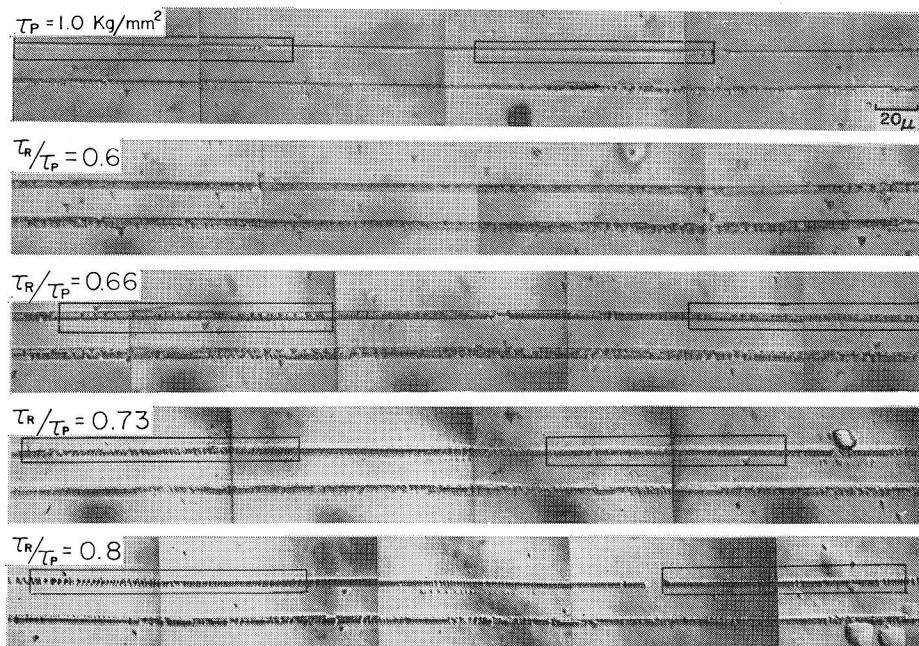


Fig. 18. Changes in dislocation configuration during reverse stressing in specimen No.2. Counting the number of pits was performed in the areas outlined.

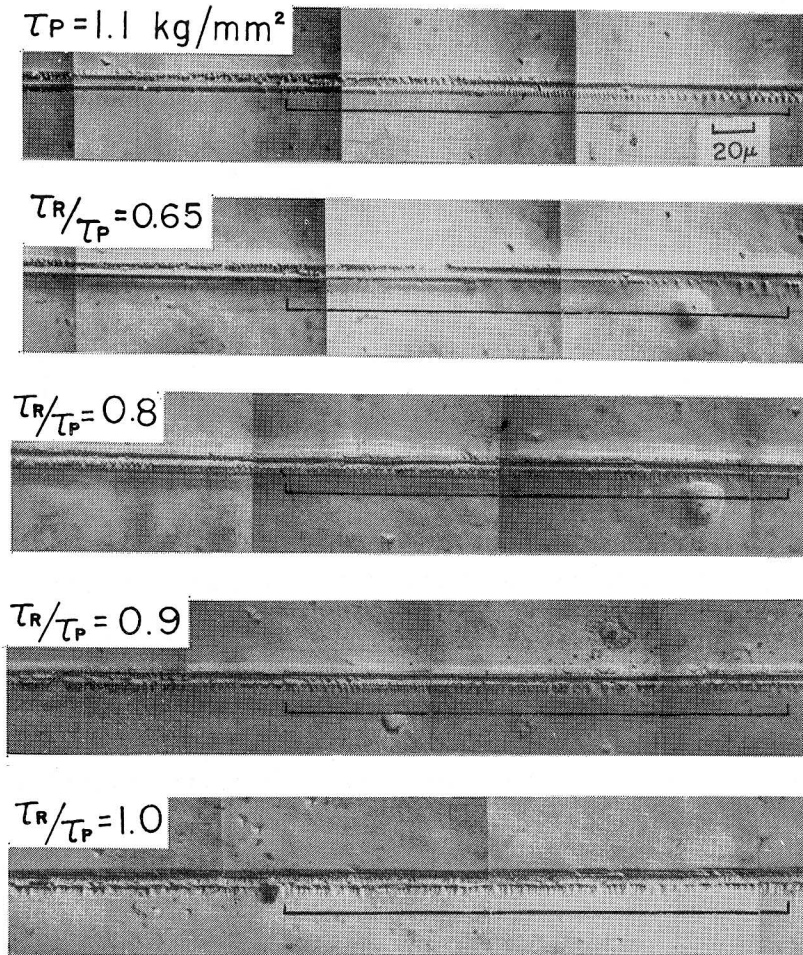


Fig. 19. Change in dislocation configuration during reverse stressing in stressing in specimen No. 3. Counting the number of pits was performed in the lower row indicated. The row of pits become somewhat irregular during reverse stressing.

The changes within other dislocation groups presented previously are also demonstrated in the same figure. The results suggest that the multiplication of dislocations takes place after the reverse stressing prior to reaching the prestress level, to compensate the softening due to the annihilation of dislocations. However, from the present observations, it cannot be concluded whether the dislocation density recovers completely or not up to the stress reversal of unity.

Although a decrease in stored energy²⁶⁻²⁸⁾ and of indentation hardness^{26,29)} during the first stage of the reverse straining after the primary extension and the recovery with the following reverse strain have already been reported, the study of direct

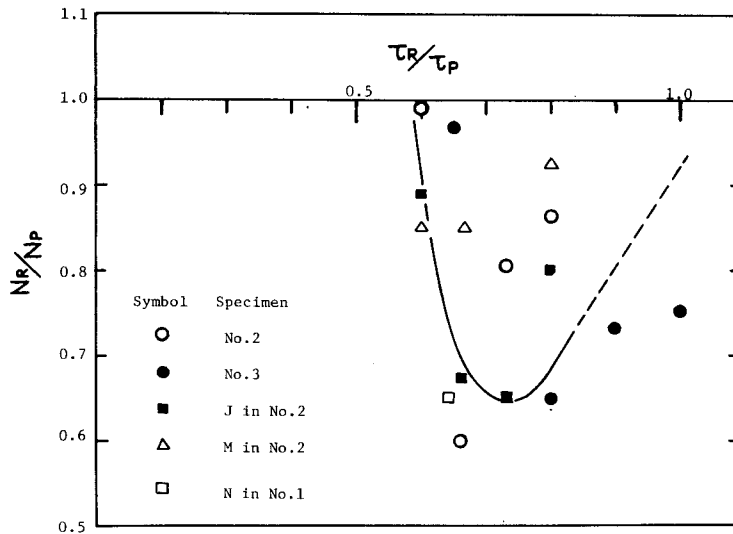


Fig. 20. Changes in dislocation density within some dislocation groups during reverse stressing: N_R and N_P indicate the number of pits under reverse stressing and that prior to reverse stressing respectively.

observations by the etch pitting method seems to be unexplored. The exception is that of annihilation at areas where rather excess dislocations are distributed inhomogeneously and locally in forms such as glide polygonization or kink band in copper^{2,3}). It is strongly believed that the previous results of indirect measurements with the Bauschinger effect can be attributed to the manifestation of the annihilation of dislocations.

The second significant aspect of the reverse behaviour was the irregular rearrangement of dislocations; i.e. the row of pits aligned in a straight line prior to the reverse stressing becomes rather irregular and complex with the reverse stressing. Consequently, the pits were not aligned in a straight line, as can be observed in Fig. 19 of specimen No. 3. It becomes evident that such an occurrence began to take advantage of the annihilation of dislocations, as can be understood from the distributions of the pits after the reverse stressing of 0.8. The occurrence of this irregularity is also observable in specimen No. 2, which is visible at the center of Fig. 16. It is therefore considered that this is a general feature due mainly to the mechanism of the annihilation of dislocations. It has been submitted that the mechanism, which is explained by the mutual annihilation of dislocations of opposite signs, emitted from a single source, is applicable to the annihilation of double ended pile-ups. However, in this case, another mechanisms is required to explain the above facts, because these rows are not considered to be double ended pile-ups, judging

from their appearances and from the irregularity of alignment during the reverse stressing.

The double cross-slip mechanism is necessary to explain these results adequately, as follows. If a cross slip of the dislocations on an adjacent glide plane takes place, these dislocations encounter the other primary dislocations of the opposite signs by the operation of a double cross slip, since this event is more favourable energetically than their reaching the dislocations of the same signs. Thus, both edge segments of the dislocation loops will attract each other and consequently be mutually annihilated. However, the edge segments of the dislocation loops which could not encounter those of the opposite signs will produce new pits when the specimen is etched. The mechnism will explain both the annihilation of dislocations aligned in the form of single ended pile-ups of the same sign, and the irregularity of rearrangements. Following the occurrence of this mechanism, it is believed that many

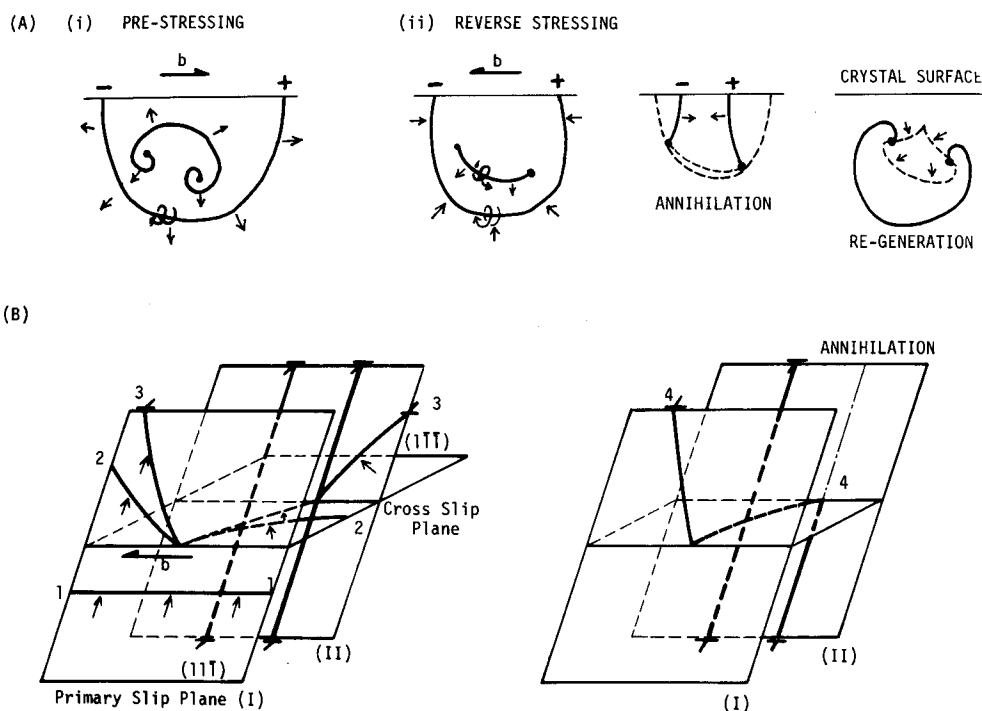


Fig. 21. Mechanisms of dislocation annihilation during reverse loading; (a) mutual annihilation of dislocations of opposite signs emitted from the same source; (b) double cross-slip mechanism, i. e., screw dislocations on primary slip plane (I) double cross slip into an adjacent primary slip plane (II). Consequently, annihilation will occur by the encounter with dislocations of opposite signs. Edge segments will be left on the cross-slip plane after the occurrence of this mechanism.

edge segments will be left on the cross slip plane. Figure 21 shows two possible mechanisms of dislocation annihilation during the reverse deformation mentioned above. In the figure, (a) is the generally accepted mechanism that is ascribed to the mutual annihilation of dislocations of opposite signs which are generated from the same source, whereas (b) is the originally proposed mechanism discussed above.

Although direct observations of dislocations in the present alloy which is deformed reversely using transmission electron microscopy, under similar conditions to this experiment, seem not to have been performed, Pande and Hazzledine⁹⁾ have reported that the densities of screws and edges remaining on the primary slip plane were similar. They also reported that many edge dislocations in the form of long multipoles sited on the cross slip plane in Cu-10at. % Al deformed unidirectionally to the end of the easy glide. Therefore, it is suggested that these screw components on a primary slip plane will provide against the operation of cross-slipping.

Koppelaar³⁰⁾ found that many cross-slip lines appear within a band at the early stage of deformation in Cu-14at. % Al single crystals, in spite of the low stacking-fault energy of the alloy. Charsley and Desvaux²¹⁾ have examined the variations of the slip line with the Bauschinger effect during reverse straining. They found that long and coarse tensile slip lines which are seen during the unidirectional deformation become shorter and finer during reverse straining. They also often terminated at cross-slip traces; and they pointed out that cross-slip had taken place actively during the reverse straining. The present observations and the proposed mechanism for the annihilation and rearrangement of dislocations are in agreement with those facts given by other investigators.

4. Conclusions

The response of dislocations on a lightly deformed Cu-9at. % Al single crystal to reverse stressing, based upon the present observations by an etch pitting technique, may be summarized as follows:

- 1) The fact that dislocations produced by pre-stressing and retained on a primary glide plane begin to move backward at the reverse stress ratio of 0.55 was confirmed by etch-pit and slip line observations. From the results, the frictional stress of dislocations of this alloy is estimated to be about 0.8 kg/mm², which is $\simeq 4/5$ of the easy glide stress.
- 2) Piled-up dislocations against a barrier and an isolated dislocation group move well under the reverse stress range from 0.6 to 0.7 to the pre-stress level, and then hardly move more than the reverse stress of 0.8.
- 3) The annihilation of dislocations begins at the same time as the occurrence of

the reverse motion of dislocations, and it takes place predominantly with increasing reverse stress. Then, gradual recovery becomes manifest up to the pre-stress level.

4) Evidence of an almost complete annihilation of double-ended pile-ups by the operation of a single dislocation source, and a partial annihilation of dislocations in uniformly aligned dislocation groups of the same signs and their irregular rearrangements were presented. Mechanisms acceptable to explain such results were proposed; i. e., the mutual annihilation of dislocations of opposite signs, and the double cross-slip mechanism.

References

- 1) G. Vellaikal; *Acta Met.*, **17**, 1145 (1969).
- 2) R. C. Daniel and G. T. Horne; *Met. Trans.*, **2**, 1161 (1971).
- 3) K. Marukawa and T. Sanpei; *Acta Met.*, **19**, 1169 (1971).
- 4) A. Howie and P. R. Swann; *Phil. Mag.*, **6**, 1215 (1961).
- 5) P. R. Thornton, T. E. Mitchell and P. B. Hirsch; *Phil. Mag.*, **7**, 1349 (1962).
- 6) R. E. Smallman and D. Green; *Acta Met.*, **12**, 145 (1964).
- 7) R. E. Smallman and K. H. Westmacott; *Phil. Mag.*, **2**, 669 (1957).
- 8) J. W. Steeds and P. M. Hazzledine; *Disc. Faraday Soc.*, **38**, 103 (1964).
- 9) C. S. Pande and P. M. Hazzledine; *Phil. Mag.*, **24**, 1039 (1971).
- 10) C. S. Pande and P. M. Hazzledine; *Ibid.*, **24**, 1393 (1971).
- 11) C. E. Feltner and C. Laird; *Acta Met.*, **15**, 1633 (1967).
- 12) R. L. Segall, J. M. Finney; *Acta Met.*, **11**, 685 (1963).
- 13) J. C. Grosskreutz, W. H. Reimann and W. A. Wood; *Acta Met.*, **14**, 1549 (1966).
- 14) D. H. Avery and W. A. Backofen; *Fracture of Solids*, Interscience, New York, p. 339 (1962).
- 15) D. H. Avery and W. A. Backofen; *Acta Met.*, **11**, 653 (1963).
- 16) J. W. Mitchell, J. C. Chevrier, B. J. Hockey and J. P. Monaghan; *Can. J. Phys.*, **45**, 453 (1966).
- 17) B. J. Hockey and J. W. Mitchell; *Phil. Mag.*, **26**, 409 (1972).
- 18) S. Yoshioka, Y. Nakayama and T. Ito; *J. Japan Inst. Met.*, **11**, 1071 (1965).
- 19) J. D. Livingston; *Acta Met.*, **10**, 229 (1962).
- 20) J. D. Livingston; *Direct Observations of Imperfections in Crystal*, Interscience, New York, p. 116 (1962).
- 21) P. Charsley and M. P. E. Desvaux; *Mater. Sci. Eng.*, **4**, 211 (1969).
- 22) A. H. Cottrell; *Dislocations and Plastic Flow in Crystals*, Oxford, p. 111 (1953).
- 23) J. D. Meakin and H. G. F. Wilsdorf; *Trans. AIME*, **218**, 745 (1960).
- 24) P. R. Strutt; *J. Aust. Inst. Metals*, **8**, 115 (1963).
- 25) P. R. Strutt, B. H. Kear and H. G. F. Wilsdorf; *Acta Met.*, **14**, 611 (1966).
- 26) A. S. Iyer and P. Gordon; *Trans. AIME*, **215**, 729 (1959).
- 27) M. E. Hargreaves, M. H. Loretto, L. M. Clarebrough and R. L. Segall; *Relation between Structure and Mechanical Properties of Metals*, (London H. M. S. O.), p. 209 (1963).
- 28) M. B. Bever, D. L. Holt and A. L. Titchener; *Progress in Materials Science*, Vol 17, Pergamon Press, p. 62 (1973).
- 29) I. Gokyu, T. Kishi and H. Wada; *J. Japan Inst. Metals*, **31**, 154 (1970).
- 30) T. J. Koppennal; *Acta Met.*, **11**, 537 (1963).